

Design Optimization of a Pole-Changing Biased Flux Machine Based on Sensitivity Analysis

Yuan Mao

Department of Electrical Engineering
The Hong Kong Polytechnic University
Hong Kong
yuan.my.mao@connect.polyu.hk

Shuangxia Niu

Department of Electrical Engineering
The Hong Kong Polytechnic University
Hong Kong
eesxniu@polyu.edu.hk

Weinong Fu

Department of Electrical Engineering
The Hong Kong Polytechnic University
Hong Kong
eewnfu@polyu.edu.hk

Abstract—In this paper, a novel pole-changing biased flux machine is proposed. With special rotor pole and permanent magnetic pole design, this machine has pole-changing effect. By controlling the excitation current's polarity the pole number of this machine can switch back and forth between three pole pair and six pole pair. The armature winding is designed in concentrated structure to realize higher utilization ratio of flux linkage under both pole modes. To further improve the performance of the proposed machine, topology optimization is conducted. In order to verify the feasibility of this design, electromagnetic characteristics, including coil flux linkage distribution, air gap flux density and harmonics analysis are studied under finite element method.

Keywords—biased flux machine, finite element method, permanent magnet machine, pole-changing, sensitivity analysis

I. INTRODUCTION

Biased flux machine (BFM) have attracted increasing attention in the area of electric machine recently. The phenomenon of biased flux can be traced to half a century ago in double salient permanent magnet (PM) machine [1] as well as the switching reluctance machine proposed afterwards [2]. However, this phenomenon has not drawn researchers' attention for a long time until the author in [3] presented a systematic study of BFM. By definition, BFM refers to the machine which has biased flux in armature coils [4]. With specific design of machine's rotor pole and slot combination, the flux polarity of stator coils will keep unaltered no matter where the rotor position is, which is called the biased flux effect [5].

The biased flux effect indicates that there are three degrees of freedom to control the BFM. In addition to the ordinary control strategy with AC component amplitude and phase, the DC component amplitude is also a control method. Inspired by the biased flux effect, a number of DC current excited hybrid biased flux machines are proposed in recent years' literatures. In [6] the hybrid-excited BFM with slot PM-assisted structure is proposed. This machine design is derived from traditional doubly-salient structure, which employs an additional DC field winding in the slots. Moreover, an improved design with segmented stator and rotor is presented in [7], which can eliminate the phase shift due to the asymmetric saturation of the magnetic path. The author in [8] presented another thinking which fulfilled flux control by injecting a current pulse in memory magnetic material. However, the above mentioned hybrid-excited machines have the same feature that they all followed the concept of series hybrid excitation. Series hybrid excitation (SHE), as the name implies, is that the excitation field and the PM field share the same magnetic circuit. The field current is used to enhance or weaken the PM field. The SHE is the most common design method for hybrid-excited

machine. However, SHE design method may suffer from some limitations. To name a few, long-term magnetization strengthening and weakening may cause magnets' demagnetization and high level of field current may get close to saturation. In contrast, parallel hybrid excitation (PHE) machine have less risks to face these problems for the reason that the flux path of field excitation and the PM excitation will not overlap in PHE machine.

Pole-changing machine is a type of PHE machine. The pole-changing permanent magnet (PCPM) machine was first proposed in [9], which applies the memory motor technique to alter the pole number. In [10] the author proposed a variable flux pole-changing machine, which had higher winding utilization than the PCPM machine by adopting fractional-slot concentrated winding. Afterwards, the author in [11] presented a dual-memory pole-changing machine, which adopted both the neodymium-iron-boron (Nd-Fe-B) PM and also the aluminum-nickel-cobalt (Al-Ni-Co) PM together to achieve effective flux control. Nevertheless, these designs use memory magnetic materials invariably, which have limitations in practical applications. To name a few, the detailed magnetization level of mnemonic magnet material is hard to be determined and meanwhile the transient process in control the magnetization direction of memory material is complex.

In this paper, a novel pole-changing biased flux (PCBF) machine is proposed. This machine adopts the PHE strategy and Nd-Fe-B PM material, which has less risk in demagnetization than mnemonic magnet material [12]. In addition, this machine maintains the partitioned stator structure which could improve the torque density by further enhancing the space utilization [13]. To further improve the performance of this machine, topology optimization based on sensitivity analysis is conducted. The sensitivity analysis is combined with Taguchi method which can greatly reduce the computation cost by selecting near-optimal parameters [14].

II. MACHINE CONFIGURATION AND WORKING PRINCIPLE

Fig. 1 shows the cross section configuration of the proposed PCBF machine. It has partitioned stator structure, which moves the PMs from the traditional primary stator into the inner stator. The outer stator has concentrated armature winding wound in the slot. The inner stator has field winding wound in the slot. It should be noted that the circling directions of adjacent field coils are opposite. All the PMs are radially magnetized and adjacent PMs have opposite magnetization directions as illustrated by the arrows in Fig. 1.

This structure is a typical biased flux machine, which has unipolar flux linkage in each coil. Fig. 2 is a schematic figure to illustrate the feature of biased flux effect in this

machine. The red waveform corresponds to the coil close to the red PM segment while the blue waveform corresponds to the blue one. When the rotor moves at position 1 and position 2, the flux linkage presents as the arrow points. When the rotor keeps moving, the flux linkages keep changing and appear like sinusoidal waves. It can be seen that the relative position of PM poles and coils are fixed. With the motivation of ferrite segments of rotor, the magnitude of flux linkages in each coil changes while the direction keeps invariable. Since there is position difference between the neighboring coils, the red and blue coil flux has different phase angle.

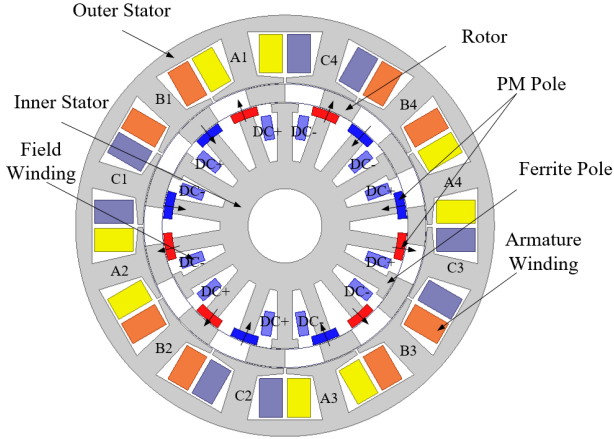


Fig. 1 Configuration of the pole-changing biased flux machine.

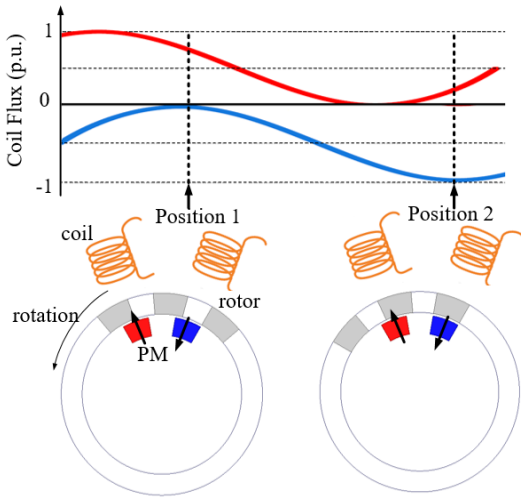


Fig. 2 Operation principle explanation of biased flux machine.

In essence the proposed PCBF machine belongs to the flux-modulation machine [15]. The electromagnetic mechanism also obeys the flux-modulation effect [16]. The pole pair numbers and rotational speeds of magnetic harmonics components fulfill the flux modulation theory, which can be expressed as,

$$\begin{cases} p_{m,k} = |mp_{MS} + kN_r| \\ \omega_{m,k} = \frac{mp_{MS}}{mp_{MS} + kN_r} \omega_{MS} + \frac{kN_r}{mp_{MS} + kN_r} \omega_m \\ m = 1, 3, 5, 7 \dots \quad k = 0, \pm 1, \pm 2 \dots \end{cases} \quad (1)$$

where p_{MS} is the pole pair number of PM, N_r is the number of rotor segments, m is the corresponding order of Fourier

series, ω_m is the rotation speed of rotor, ω_{MS} is the rotation speed of stator PM.

The BFM, as a unique classification of flux-modulation machine, should also fulfill the distinct slot/stator pole combination conditions. Only the flux-modulation machines with all coils underneath one single PM pole could be transferred to BFMs [17]. This means the slot number N_s could be divided by the PM pole pair number p_{MS} . Besides, since the coils are divided into two groups with negative and positive biased flux symmetrically, the slot number N_s must be an even number. Meanwhile considering the phase number of machines, the slot number N_s should also be dividable by phase number q . Thus the BFM slot/stator pole combination standard could be governed by the following formulas:

$$\begin{cases} N_s = 2aq \quad a = 1, 2, 3 \dots \\ p_{MS} = \{b | \text{mod}(N_s, 2b) = 0 \quad b = 1, 2, 3 \dots\} \end{cases} \quad (2)$$

Considering the above formulas, the potential slot/stator pole combination of three phase BFMs could be summarized as listed in Table I.

TABLE I. POTENTIAL SLOT/STATOR POLE PAIR COMBINATION OF THREE PHASE BFM

Slot Number N_s	Stator Pole Pair Arrangement	
	Stator Pole Pair Number p_{MS}	N_s/p_{MS}
6	1	6
	3	2
12	1	12
	2	6
	3	4
	6	2
6a (a=1,2,3)	$\{b \text{mod}(N_s, 2b) = 0 \quad b = 1, 2, 3 \dots\}$	N/A

III. POLE-CHANGING OPERATION ANALYSIS

In section II, the potential slot/stator combinations of BFMs have been summarized. Based on the stator/slot combinations listed in Table I, the pole pair number in each operation mode should also obey the standard. It can be found that under the condition of 12 slots number, the potential stator PM pole pair number can be 1,2,3,6. Therefore the pole-changing mode with 3/6 pole pair arrangement is selected in this design. The performance of pole-changing machine with 1/3 pole pair arrangement is unsatisfactory, which is not discussed in this study.

The basic principle of the PCBF machine is to change the effective PM pole pair number by magnetic flux cancellation of a certain PM pole, which is equivalent to discarding the PM magnetic pole [11]. In normal operation mode of the PCBF machine, its ferrite pole is magnetized by the DC field winding. In flux-weakening mode, there is no DC current injected in the field winding of the PCBF machine. The flux line distribution figure is tested by finite element method (FEM) and shown in Fig. 3. Distinct pole-changing phenomenon can be observed in the figure with or

without DC field current applied. To further clarify the pole-changing effect in this machine, the air gap flux density waveform is also simulated and plotted in Fig. 4. The simulation is done under no-load condition with the inject DC current at 15A and 30 turns. The results show that the ferrite poles have flux lines distributed at normal mode while little flux lines distributed at flux-weakening mode. The airgap flux density also shows different flux distribution at both modes. There exists a field excitation flux waveform between two PM excitation waveform in normal mode. The back electromotive force (EMF) is also tested and plotted in Fig. 5. It can be seen that the back EMF can be reduced from about 40V to 20V after pole changing. To conclusion, the PCBF machine has a relatively wide flux control range with low input field current.

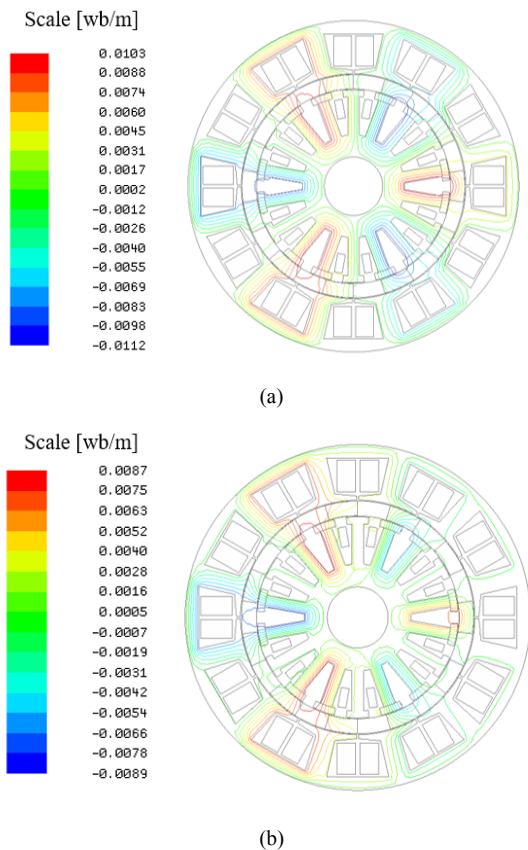


Fig. 3 Flux line distribution of PCBF machine at (a) normal mode (b) flux weakening mode.

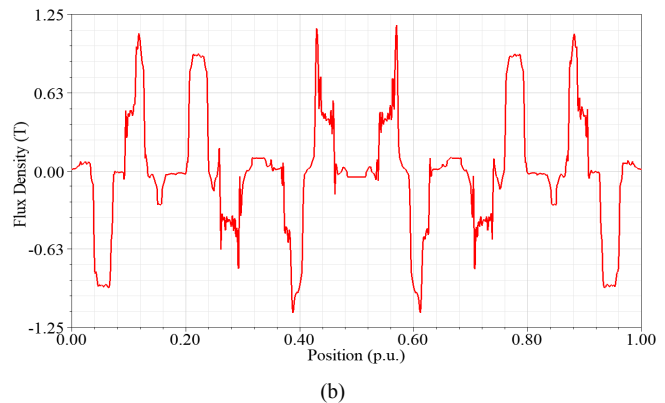
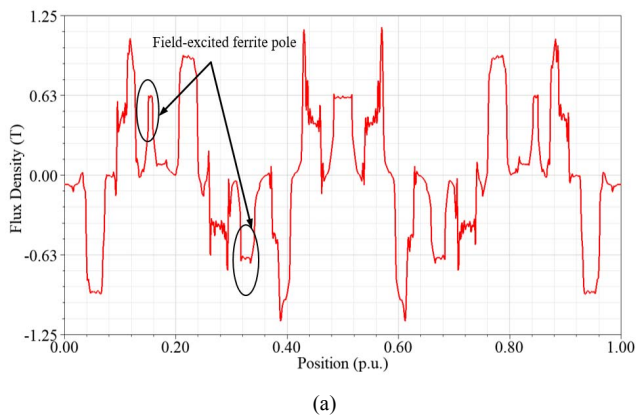


Fig. 4 Flux density of PCBF machine at (a) normal mode (b) flux weakening mode

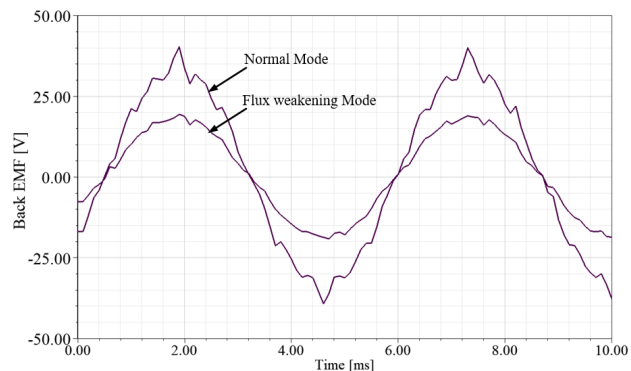


Fig. 5 Back EMF of PCBF machine at normal mode and flux weakening mode

IV. SENSITIVITY ANALYSIS AND OPTIMIZATION

Topology optimization is essential in machine design which may conduce to higher performance and lower economic costs. However, it is time consuming to deal with machine optimization. In general, electromagnetic characteristics of electric machine cannot be expressed by several simple equations. Therefore, finite element analysis (FEA) is widely used in machine analysis. In order to further reduce the computation time, this study reasonably reduces some design parameters by examining the sensitivity factors. Taguchi method provides the theoretical foundation to the sensitivity analysis in this study.

The establishment of the Taguchi method is based on the principle of the orthogonal array method, which can effectively reduce the number of design experiments required in the design process. The Taguchi method can provide an effective method for obtaining optimal parameters in optimization problems with as few experiments as possible. The Taguchi method uses the orthogonal array method to study the influence of parameter changes [18]. This paper resorts to the Taguchi method to determine the approximate optimal value of the design variables by means of analysis of variance (ANOVA). The detailed analysis is presented as sub sections below.

A. Establishment of Optimization Variables and Cost Functions

The initial values of design parameters are shown in Table II. Among them, $\mathbf{x}=\{a_{PM}, h_{int}, h_{PM}, h_r, h_{s2}, b_s, w_{int}, R_{ins}\}$ can be the optimization variable array while other parameters are set as constant. The objective of optimization

is to maximize electromagnetic torque ($T(\mathbf{x})$) under normal operation mode. During optimization the current density of armature winding should be restricted in a value. However, in optimization process, the area of slot ($S(\mathbf{x})$) always changes. As known to all, $S(\mathbf{x})$ is in proportional to the amplitude of input current I under certain current density δ and the electromagnetic torque $T(\mathbf{x})$ is in proportional to the input current I . Therefore the objective function $C(\mathbf{x})$ can be equivalent provided that multiples output torque $T(\mathbf{x})$ by the per unit value of $S(\mathbf{x})$, that is,

$$C(\mathbf{x}) = \max(T(\mathbf{x}) * S(\mathbf{x}) / S_{initial}) \quad (3)$$

where $S_{initial}$ represents the initial slot area.

TABLE II. DESIGN PARAMETERS AND INITIAL VALUE

Symbol	Meaning	Initial Value	constant or variable
D	outer diameter	170(mm)	constant
R_{shaft}	shaft radius	15(mm)	constant
l	axial length	65(mm)	constant
ag	air gap length	0.5(mm)	constant
δ	current density	5.5(A/mm ²)	constant
R_{ins}	inner radius	24(mm)	variable
h_{int}	inner teeth height	20(mm)	variable
h_{PM}	PM height	3(mm)	variable
h_r	rotor height	7(mm)	variable
h_{s0}	height of slot notch	2(mm)	constant
h_{s1}	height of slot top	1(mm)	constant
h_{s2}	height of slot	15(mm)	variable
bs_0	width of slot notch	1(mm)	constant
bs	width of slot	24(mm)	variable
w_{int}	inner teeth width	7(mm)	variable
a_{PM}	PM arc angle	6(deg)	variable

B. Establishment of Taguchi Orthogonal Array

One common and intuitional method to examine the sensitivity factors in an optimization study is the full factorial method. As mentioned above, 8 parameters are required to be optimized in this study. If each parameter is examined with three levels, it requires 8^3 , which equals to 512 experiments using the full factorial method. That is an extremely large project. The Taguchi method is a reasonable means to reduce the number of experiments. Not all of the possible parameter combinations are tested, but some selected combinations. The way to decide which combination to be considered is resorted to the Taguchi Orthogonal Array (TOA).

Considering time cost and accuracy requirement, the L18 TOA is relative suitable for this study. The level arrangement of each variable is shown in Table III. According to the L18 TOA, the 18 experiments and results are listed in Table IV.

C. Establishment of ANOVA

To analyze the influence of each factor, the analysis of means (ANOM) and ANOVA are conducted. Firstly, the average effect of each parameter in each level can be calculated by ANOM. The results are presented in Table V. Secondly, the near optimal parameter level is concluded.

The parameter at level combination array $\mathbf{L} = (L_1, L_3, L_2, L_2, L_3, L_1, L_2, L_2)$ contributes to the most optimal value, which corresponds to the near optimal solution of each parameter. Thirdly, ANOVA of each factor is conducted to measure the derivation from the mean value. In the end, the proportion of the derivation of each parameter is derived which reveals the factor effects. The factor effects results are shown in Table VI.

TABLE III. OPTIMIZATION PARAMETERS LEVEL ARRANGEMENT

Parameter	Level 1 (L1)	Level 2 (L2)	Level 3 (L3)
a_{PM}	6(deg)	8(deg)	N/A
h_{int}	10(mm)	15(mm)	20(mm)
h_{PM}	2(mm)	3(mm)	4(mm)
h_r	5(mm)	7(mm)	9(mm)
h_{s2}	12(mm)	15(mm)	18(mm)
bs	24(mm)	28(mm)	32(mm)
w_{int}	4(mm)	6(mm)	8(mm)
R_{ins}	24(mm)	28(mm)	32(mm)

TABLE IV. TAGUCHI ORTHOGONAL ARRAY

No.	Level Combinations							
	a_{PM}	h_{int}	h_{PM}	h_r	h_{s2}	bs	w_{int}	R_{ins}
1	L1	L1	L1	L1	L1	L1	L1	L1
2	L1	L1	L2	L2	L2	L2	L2	L2
3	L1	L1	L3	L3	L3	L3	L3	L3
4	L1	L2	L1	L1	L2	L2	L3	L3
5	L1	L2	L2	L2	L3	L3	L1	L1
6	L1	L2	L3	L3	L1	L1	L2	L2
7	L1	L3	L1	L2	L1	L3	L2	L3
8	L1	L3	L2	L3	L2	L1	L3	L1
9	L1	L3	L3	L1	L3	L2	L1	L2
10	L2	L1	L1	L3	L3	L2	L2	L1
11	L2	L1	L2	L1	L1	L3	L3	L2
12	L2	L1	L3	L2	L2	L1	L1	L3
13	L2	L2	L1	L2	L3	L1	L3	L2
14	L2	L2	L2	L3	L1	L2	L1	L3
15	L2	L2	L3	L1	L2	L3	L2	L1
16	L2	L3	L1	L3	L2	L3	L1	L2
17	L2	L3	L2	L1	L3	L1	L2	L3
18	L2	L3	L3	L2	L1	L2	L3	L1

TABLE V. EFFECTIVE FACTOR AND PROPORTION

Parameter	a_{PM}	h_{int}	h_{PM}	h_r	h_{s2}	bs	w_{int}	R_{ins}
effective factor	0.21	0.49	1.86	0.86	0.65	2.25	0.12	0.85
proportion (%)	2.9	6.7	25.5	11.8	8.9	30.9	1.6	11.7
selected optimization variable	no	no	yes	yes	no	yes	no	yes

D. Discussions and Comparisons

From the ANOVA results, it can be concluded that the parameter *bs* in topology design, has the highest effect on the output torque while the parameter *wint* is the lowest effective factor. To lower the calculation in optimization, the factors that have lower effective factor can be eliminated. In this study, *hPM*, *hr*, *bs* and *Rins* are selected as variables in the next step of optimization. The other four parameters use the near optimal solution as approximations. To be compared, optimization involved full parameters is also conducted. The Differential Revolution (DE) algorithm based on FEA is adopted in optimization [19-21]. The cost value under the full parameter optimization is 8.87 and 8.85 in reduced parameter optimization. In addition, the near optimal cost value using level combination $L=(L1, L3, L2, L2, L3, L1, L2, L2)$ is 8.73. The difference of full parameter optimization between three parameter optimization is less than 1%. It is worth noting that the error is less than 2% for the near optimal solution using Taguchi method. The overall computing time of reduced parameters optimization is reduced to less than half of the full parameters optimization. Therefore, the reduced parameter optimization even the near optimal solution can be applied in some situations to save computation time [22].

TABLE VI. OPTIMIZATION PARAMETERS LEVEL ARRANGEMENT

	Full parameter optimization	Reduced parameter optimization
Individuals	50	25
Generation	18	12
Optimized Parameters	<i>aPM</i> =6.5(deg)	<i>aPM</i> (L1)
	<i>hint</i> =19.7(mm)	<i>hint</i> (L3)
	<i>hPM</i> =3.5(mm)	<i>hPM</i> =3.2(mm)
	<i>hr</i> =7.2(mm)	<i>hr</i> =7.3(mm)
	<i>hs2</i> =17.6(mm)	<i>hs2</i> (L3)
	<i>bs</i> =26.6(mm)	<i>bs</i> =25.7(mm)
	<i>wint</i> =6.0(mm)	<i>wint</i> (L2)
	<i>Rins</i> =26.3(mm)	<i>Rins</i> =26.5(mm)
Cost Value	8.87	8.85

V. CONCLUSION

This paper mainly describes the design, performance and optimization of the PCBF machine. PCBF machine has parallel excitation structure which can avoid irreversible demagnetization in series excitation design. This machine can operate at normal mode and flux weakening mode by injecting field current. The electromagnetic performance of the PCBF machine is tested and presented. It results in a wide range of flux weakening control. Considering the complexity of the electromagnetic characteristics of the motor, its response cannot be expressed simply by formulas. Therefore, the optimization based on FEA experiments are commonly applied which is time-consuming. To solve this problem, a method to simplify the variables in optimization is presented. Combined Taguchi method with ANOVA, the effective factor of each design parameters can be derived. According to the factor effects, four out of eight variables are selected in optimization. The results show the simplified optimization has less than 1% difference but save more than

half time of calculation time. Furthermore, the error of the near optimal value using Taguchi method is less than 2%. Therefore, the method used in this paper may be effectively applied to the simplification of motor optimization.

ACKNOWLEDGMENT

This work was supported in part by the National Natural Science Foundation of China under Project 51707171 and in part by The Hong Kong Polytechnic University, Hong Kong, under Project PolyU 152509/16 and Project PolyU 152058/17E.References

REFERENCES

- [1] T. Sheng, S. Niu, and S. Yang, "A novel design method for the electrical machines with biased dc excitation flux linkage," *IEEE Trans. Magn.*, vol. 53, no. 6, Jun. 2017, Art. no. 8103604.
- [2] Y. Liao, F. Liang, and T. A. Lipo, "A novel permanent magnet motor with doubly salient structure," *IEEE Trans. Ind. Appl.*, vol. 31, no. 5, pp. 1069-1078, Sep./Oct. 1995.
- [3] T. Sheng, S. Niu, W. Fu and Q. F. Lin, "Topology Exploration and Torque Component Analysis of Double Stator Biased Flux Machines Based on Magnetic Field Modulation Mechanism," *IEEE Trans. Energy. Convers.*, vol. 33, no. 2, pp. 584-593, Jun. 2018.
- [4] M. Y. Lin, M. Cheng, and E. Zhou, "Design and performance analysis of new 12/8-pole doubly salient permanent-magnet motor," in *Proc. 6th Int. Conf. Electron. Mach. Syst.*, vol. 1. Beijing, China, Nov. 2003, pp. 21-25.
- [5] X. Zhao, S. Niu, W. N. Fu, "Design of a Novel Parallel-Hybrid-Excited Dual-PM Machine Based on Armature Harmonics Diversity for Electric Vehicle Propulsion," *IEEE Trans. Ind. Elec.*, vol. 66 No. 6, pp. 4209-4219, Jun. 2019.
- [6] I. A. A. Afinowi, Z. Q. Zhu, Y. Guan, J. C. Mipo, P. Farah, "Hybrid-excited doubly salient synchronous machines with permanent magnets between adjacent salient stator poles," *IEEE Trans. Magn.*, vol. 51, no. 10, Oct. 2015.
- [7] C.H.T. Lee, J.L. Kirtley, M. A. Angle, "Partitioned-stator flux-switching permanent-magnet machine with mechanical flux adjusters for hybrid electric vehicles," *IEEE Trans. Magn.* vol. 53, pp.3000807, 2017.
- [8] H. Liu, H. Lin, Z. Q. Zhu, M. Huang, and P. Jin, "Permanent magnet remagnetizing physics of a variable flux memory motor," *IEEE Trans. Magn.*, vol. 46, no. 6, pp. 1679-1682, Jun. 2010.
- [9] V. Ostovic, "Pole-changing permanent-magnet machines," *IEEE Trans. Ind. Appl.*, vol. 38, no. 6, pp. 1493-1499, Nov./Dec. 2002.
- [10] C. Yu and K. T. Chau, "Design, analysis, and control of DC-excited memory motors," *IEEE Trans. Energy Convers.*, vol. 26, no. 2, pp. 479-489, Jun. 2011.
- [11] F. Li, K.T. Chau, C. Liu, "Pole-changing flux-weakening DC-excited dual-memory machines for electric vehicles," *IEEE Trans. Energy Convers.*, vol. 31, pp. 27-36, 2016.
- [12] X. Zhao, S. Niu, W. N. Fu, "Development of a Novel Transverse Flux Tubular Linear Machine With Parallel and Complementary PM Magnetic Circuit for Precision Industrial Processing," *IEEE Trans. Ind. Elec.*, vol. 66 No. 6, pp. 4945-4955, Jun. 2019.
- [13] Z. Z. Wu and Z. Q. Zhu, "Partitioned stator flux reversal machine with consequent-pole pm stator," *IEEE Trans. Energy. Convers.*, vol. 30, no. 4, pp. 1472-1482, Dec. 2015.
- [14] C. C. Hwang, L. Y. Lyu, C. T. Liu, and P. L. Li, "Optimal design of an SPM motor using genetic algorithms and Taguchi method," *IEEE Trans. Magn.*, vol. 44, no. 11, pp. 4325-4328, Nov. 2008.
- [15] D. Li, Y. Gao, R. Qu, J. Li, Y. Huo and H. Ding, "Design and analysis of a flux reversal machine with evenly distributed permanent magnets," *IEEE Trans. Ind. Appl.*, vol. 54, no. 1, pp. 172-183, Jan.-Feb. 2018.
- [16] Y. Liu, S. Niu, and W. Fu, "A novel multiphase brushless power-split transmission system for wind power generation," *IEEE Trans. Magn.*, vol. 52, no. 2, pp. 1-7, Feb. 2016.
- [17] M. Yuan and S. Niu, "Design and analysis of a novel modular linear double-stator biased flux machine," *IEEE Trans. Magn.*, vol. 54, no. 11, pp. 1-5, Nov. 2018.
- [18] H. M. Hasaniien, "Design optimization of PID controller in automatic voltage regulator system using Taguchi combined genetic algorithm method," *IEEE Syst. Journal*, vol. 7, no. 4, pp. 825-831, Dec. 2013.

- [19] Y. Mao, S. Niu, and Y. Yang, "Differential evolution-based multiobjective optimization of the electrical continuously variable transmission system," *IEEE Trans. Ind. Elec.*, vol. 65, no. 3, pp. 2080–2089, 2018.
- [20] S. Saponara, P. Tisserand, P. Chassard, D. M. Ton, "Design and measurement of integrated converters for belt-driven starter-generator in 48 V micro/mild hybrid vehicles", *IEEE Trans. Ind. Appl.*, vol. 53, no. 4, pp. 3936-3949, Jul./Aug. 2017.
- [21] Y. Yang, S. Tan and S. Y. Hui, "Front-end parameter monitoring method based on two-layer adaptive differential evolution for SS-compensated wireless power transfer systems," *IEEE Trans. on Ind. Informat.*, Jun. 2019, Early Access.
- [22] M. Ashabani, Y. Abdel-Rady, I. Mohamed, and J. Milimonfared, "Optimum design of tubular permanent-magnet motors for thrust characteristics improvement by combined Taguchi-neural network approach," *IEEE Trans. Magn.*, vol. 46, no. 12, pp. 4092-4100, Dec. 2010.